

# Liver-Specific siRNA-Mediated Stat3 or C3 Knockdown Improves the Outcome of Experimental Autoimmune Myocarditis

Lidia Avalle,<sup>1,7</sup> Francesca Marino,<sup>1,7</sup> Annalisa Camporeale,<sup>1</sup> Chiara Guglielmi,<sup>1,8</sup> Daniele Viavattene,<sup>1</sup> Silvio Bandini,<sup>1</sup> Laura Conti,<sup>1</sup> James Cimino,<sup>1</sup> Marco Forni,<sup>2</sup> Cristina Zanini,<sup>2</sup> Alessandra Ghigo,<sup>1</sup> Roman L. Bogorad,<sup>3</sup> Federica Cavallo,<sup>1</sup> Paolo Provero,<sup>1,4</sup> Victor Koteliansky,<sup>5,6</sup> and Valeria Poli<sup>1</sup>

<sup>1</sup>Department of Molecular Biotechnology and Health Science, University of Torino, Via Nizza 52, Torino 10126, Italy; <sup>2</sup>EuroClone S.p.A Research Laboratory, Molecular Biotechnology Center, University of Turin, Torino 10126, Italy; <sup>3</sup>David H. Koch Institute for Integrative Cancer Research, Massachusetts Institute of Technology, Cambridge, MA 02142, USA; <sup>4</sup>Center for Translational Genomics and Bioinformatics, IRCCS San Raffaele Scientific Institute, 20132 Milan, Italy; <sup>5</sup>Skolkovo Institute of Science and Technology, Skolkovo, Moscow 121205, Russia; <sup>6</sup>Department of Chemistry, MV Lomonosov Moscow State University, Moscow 119991, Russia

**Myocarditis can lead to autoimmune disease, dilated cardiomyopathy, and heart failure, which is modeled in the mouse by cardiac myosin immunization (experimental autoimmune myocarditis [EAM]). Signal transducer and activator of transcription 3 (STAT3) systemic inhibition exerts both preventive and therapeutic effects in EAM, and STAT3 constitutive activation elicits immune-mediated myocarditis dependent on complement C3 and correlating with activation of the STAT3-interleukin 6 (IL-6) axis in the liver. Thus, liver-specific STAT3 inhibition may represent a therapeutic option, allowing to bypass the heart toxicity, predicted by systemic STAT3 inhibition. We therefore decided to explore the effectiveness of silencing liver Stat3 and C3 in preventing EAM onset and/or the recovery of cardiac functions. We first show that complement C3 and C5 genetic depletion significantly prevents the onset of spontaneous myocarditis, supporting the complement cascade as a viable target. In order to interfere with complement production and STAT3 activity specifically in the liver, we took advantage of liver-specific Stat3 or C3 small interfering (si)RNA nanoparticles, demonstrating that both siRNAs can significantly prevent myocarditis onset and improve the recovery of heart functions in EAM. Our data demonstrate that liver-specific Stat3/C3 siRNAs may represent a therapeutic option for autoimmune myocarditis and suggest that complement levels and activation might be predictive of progression to dilated cardiomyopathy.**

## INTRODUCTION

Myocarditis is an inflammatory heart disease in which its etiology is often linked to infection with viral pathogens exhibiting a direct myopathic effect. It can cause acute or chronic heart failure and progress to dilated cardiomyopathy (DCM) in susceptible individuals (about 30% of patients), representing a relatively frequent cause of cardiac failure, particularly in young adults.<sup>1</sup> Nevertheless, the basis for differential susceptibility to disease progression is not yet under-

stood. Affected hearts display abundant infiltrating myeloid cells and cluster of differentiation 4<sup>+</sup> (CD4<sup>+</sup>) T lymphocytes, and the disease is characterized by a potent T cell-mediated immune response sustaining high titers of autoantibodies against heart proteins.<sup>2</sup> Although the autoimmune pathogenesis of the chronic disease is widely accepted, despite the success obtained with immunosuppressant therapies in a subset of patients,<sup>3,4</sup> no such therapeutic protocol has yet been formally approved.

Immune-mediated myocarditis is mainly modeled in susceptible strains of mice by experimental autoimmune myocarditis (EAM),<sup>5,6</sup> where immunization with an alpha-myosin peptide, emulsified with complete Freund's adjuvant, triggers an initial acute activation of innate immunity.<sup>7</sup> This consists of abundant leukocyte infiltration in the myocardium, which is, in turn, required for the ensuing adaptive immune response.<sup>7,8</sup> Adaptive immunity is mainly driven by antigen-specific T cells and characterized by significant self-reactive antibodies production and immunoglobulin (Ig) deposition on cardiac cells,<sup>8</sup> correlating with the onset and progression of systolic dysfunction that can be assessed by echocardiography.<sup>7,9</sup> EAM studies, making use of inhibitors and of genetically modified mice, have demonstrated the pathogenic role of several cytokines and complement components,<sup>7</sup> serving as hypothesis-generating results for the human disease. For example, the inflammatory cytokine interleukin 6 (IL-6), which was shown to increase the number of cardiac myosin autoreactive CD4<sup>+</sup> T cells,<sup>8</sup> plays a key role in EAM, since IL-6 null mice are protected from myocarditis development,

Received 21 January 2020; accepted 19 May 2020;  
<https://doi.org/10.1016/j.omtm.2020.05.023>.

<sup>7</sup>These authors contributed equally to this work.

<sup>8</sup>Present address: Section of Molecular Genetics, Department of Laboratory Medicine, University Hospital of Pisa, Pisa 50127, Italy.

**Correspondence:** Valeria Poli, Department of Molecular Biotechnology and Health Science, University of Torino, Via Nizza 52, 10126 Torino, Italy.

**E-mail:** [valeria.poli@unito.it](mailto:valeria.poli@unito.it)

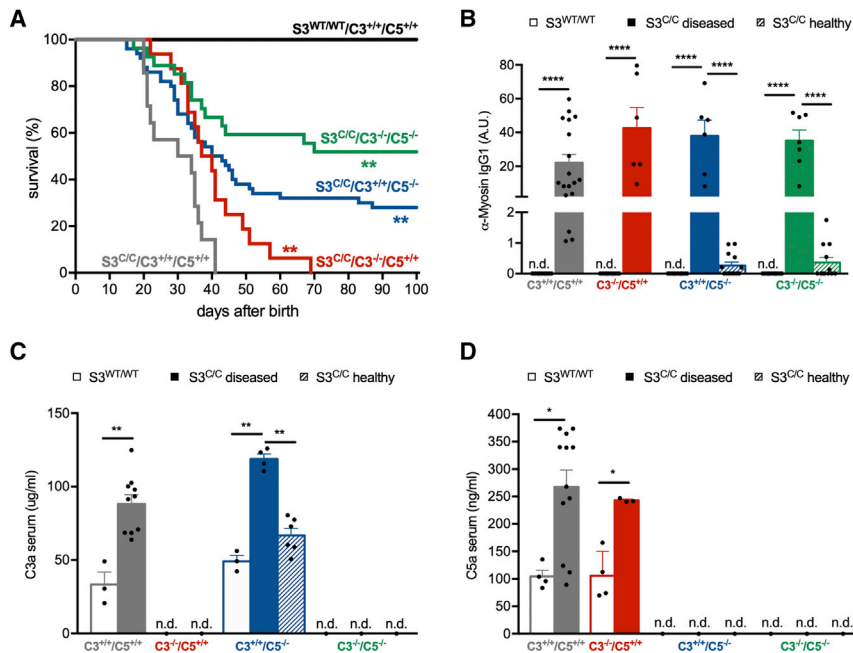


### Figure 1. Genetic Depletion of Complement C3 and C5 Rescues Myocarditis in $Stat3^{C/C}$ Mice

Mortality was recorded in mice of the indicated genotypes, followed by analysis of myocarditis-related parameters in the serum and heart. Genotypes: wild-type (WT) or homozygous for the  $Stat3$  allele ( $S3^{WT/WT}$ ,  $S3^{C/C}$ ), either sufficient or deficient for the indicated complement genes,  $C3^{-/-,+/+}$  or  $C5^{-/-,+/+}$ . (A) Kaplan Meyer curve of mice of the indicated genotypes. Log rank Mantel-Cox test, p values:  $S3^{C/C}/C3^{+/+}/C5^{+/+}$  versus  $S3^{C/C}/C3^{-/-}/C5^{-/-}$ ,  $p < 0.0001$ ;  $S3^{C/C}/C3^{+/+}/C5^{+/+}$  versus  $S3^{C/C}/C3^{-/-}/C5^{+/+}$ ,  $p = 0.0099$ ;  $S3^{C/C}/C3^{+/+}/C5^{+/+}$  versus  $S3^{C/C}/C3^{+/+}/C5^{-/-}$ ,  $p = 0.0011$ ;  $S3^{C/C}/C3^{-/-}/C5^{+/+}$  versus  $S3^{C/C}/C3^{-/-}/C5^{-/-}$ ,  $p = 0.0008$ ;  $S3^{C/C}/C3^{+/+}/C5^{-/-}$  versus  $S3^{C/C}/C3^{-/-}/C5^{-/-}$ ,  $p = 0.0490$ ; n:  $S3^{WT/WT}/C3^{+/+}/C5^{+/+}$  (black line),  $n = 64$ ;  $S3^{C/C}/C3^{+/+}/C5^{+/+}$  (gray line),  $n = 14$ ;  $S3^{C/C}/C3^{-/-}/C5^{-/-}$  (red line),  $n = 16$ ;  $S3^{C/C}/C3^{+/+}/C5^{-/-}$  (blue line),  $n = 50$ ;  $S3^{C/C}/C3^{-/-}/C5^{+/+}$  (green line),  $n = 27$ . (B) Serum anti-myosin IgG1 autoantibodies measured by ELISA at sacrifice in mice wild-type (empty bars, values below threshold),  $Stat3^{C/C}$  diseased (filled bars), or healthy (striped bars), carrying inactivated (-) C3 (red bars), C5 (blue bars), or both (green bars) genes. Data are mean  $\pm$  SEM of the indicated values. n.d., not detected. Mann-

Whitney U test, p values: \*\*\*\* $p < 0.0001$ . (C) Serum C3a measured by ELISA in the mice described in (B). (D) Serum C5a was measured as described in (C). (C and D) Data are mean  $\pm$  SEM of the indicated values. n.d., not detected. Unpaired two-tailed Student's t test with Welch's correction: \* $p < 0.05$ ; \*\* $p < 0.01$ .

correlating with reduced complement C3 expression and heart deposition.<sup>10</sup> Indeed, C3 is thought to promote EAM by activating mast cells and macrophages, triggering, in turn, autoreactive T and B cells.<sup>7,11</sup> Complement depletion by means of cobra venom factor or inactivation of the  $CR1/2$  C3 receptor genes impairs EAM induction by globally decreasing the levels of tumor necrosis factor  $\alpha$  (TNF- $\alpha$ ), IL-1 $\beta$ , and anti-myosin autoantibodies, as well as T helper cell type 1 (Th1)- and Th2-type immune responses.<sup>12</sup> IL-6, together with transforming growth factor  $\beta$  (TGF- $\beta$ ), is the major driver of Th17 cell differentiation via the activation of the transcription factor signal transducer and activator of transcription 3 (STAT3),<sup>13,14</sup> and indeed, Th17-type responses are a key adaptive immunity feature in EAM, playing a major role in postmyocarditis remodeling and DCM development.<sup>15,16</sup>

We have recently shown that STAT3 systemic inhibition could not only prevent EAM development but also therapeutically improve heart function when administered at the inflammation peak.<sup>17</sup> Moreover, ubiquitous expression of constitutively active STAT3 ( $Stat3^{C/C}$ ) in genetically modified  $Stat3^{C/C}$  mice was sufficient to elicit the development of an immune-mediated form of myocarditis, reminiscent of EAM, involving the activation of a STAT3-IL-6 axis, specifically in the liver. This conclusion was supported by increased hepatic-specific expression of the IL-6 receptor (IL-6R), in which its blockage by means of neutralizing antibodies could significantly impair the development of heart inflammation and autoimmunity.<sup>17</sup> Here, we show that complement C3 and C5 genetic depletion significantly blunts myocarditis in the  $Stat3^{C/C}$  mice, strongly supporting the pathogenic role of complement. Next, we set out to demonstrate our hypothesis

that myocarditis development in the  $Stat3^{C/C}$  mice may be triggered by the observed enhancement of IL-6 signaling in the liver, presumably via overproduction of complement components and complement-activating, acute-phase proteins. In order to prove this hypothesis, we generated liver-specific small interfering RNA (siRNA) lipidoid particles and show that interference with either STAT3 or C3 expression in the liver exerts both protective and therapeutic effects in EAM, confirming the involvement of liver inflammation in autoimmune myocarditis and suggesting a potential novel liver-targeted strategy for therapeutic intervention also in patients.

## RESULTS

### C3 and C5 Genetic Depletion Partially Rescues Myocarditis in $Stat3^{C/C}$ Mice

In order to further explore the role of complement in the immune-mediated myocarditis developing in the  $Stat3^{C/C}$  mice, we intercrossed them with mice carrying null alleles for the C3 gene,<sup>18</sup> the C5 gene,<sup>19</sup> or both, generating  $Stat3^{C/C}/C3^{-/-}$ ,  $Stat3^{C/C}/C5^{-/-}$ , and  $Stat3^{C/C}/C3^{-/-}/C5^{-/-}$  compound mutant mice. Although C3 genetic depletion significantly delayed disease development as compared with  $Stat3^{C/C}$  mice (Figure 1A; compare gray and red lines), all  $Stat3^{C/C}/C3^{-/-}$  mice eventually developed myocarditis and succumbed to the disease, displaying high levels of anti-myosin antibodies and of myeloid heart infiltration (Figures 1B and 2A). Figure S1 shows the gating used to analyze the flow cytometry data of Figure 2A. Despite the complete absence of C3, the circulating levels of activated C5 were equivalent in  $Stat3^{C/C}/C3^{-/-}$  mice and their C3-sufficient littermates (Figure 1D), suggesting activation of the complement cascade even in the absence of C3, as previously reported.<sup>20</sup> In contrast, inactivation

of the *C5* gene led to the survival of 28% of the *Stat3<sup>C/C</sup>/C5<sup>-/-</sup>* mice (Figure 1A; blue line). Surviving mice (hereafter denominated “healthy”) showed very little anti-myosin antibodies and a number of heart-infiltrating myeloid cells similar to wild-type mice (Figures 1B and 2A; striped bars), whereas mice succumbing to the disease (hereafter denominated “diseased”) were indistinguishable from their *C5*-sufficient *Stat3<sup>C/C</sup>* littermates for these parameters, as well as for the serum levels of activated C3 (Figures 1B, 1C, and 2A; filled bars). Interestingly, the inactivation of both the *C3* and *C5* genes triggered a synergic effect, affording protection from myocarditis to 52% of the mice (Figure 1A; green line). Similar to the *C5<sup>-/-</sup>* mice, healthy *C3<sup>-/-</sup>/C5<sup>-/-</sup>* double-mutant *Stat3<sup>C/C</sup>* mice displayed very low anti-myosin antibodies and no heart infiltration (Figures 1B and 2A; striped bars). Both features were instead similar to those of their *C3*, *C5*-sufficient *Stat3<sup>C/C</sup>* controls (CTRLs) in diseased mice (Figures 1B and 2A; filled bars). Confirming the null phenotype, neither activated C3 nor C5 was detectable in the double-mutant mice (Figures 1C and 1D). These results were confirmed by heart immunohistochemical analysis in mice of the different genotypes (Figures 2B and 2C). In keeping with the above observations, whereas diseased mice of all genotypes (*Stat3<sup>C/C</sup>*, *Stat3<sup>C/C</sup>/C3<sup>-/-</sup>*, *Stat3<sup>C/C</sup>/C5<sup>-/-</sup>*, and *Stat3<sup>C/C</sup>/C3<sup>-/-</sup>/C5<sup>-/-</sup>*) displayed abundant infiltration and heart fibrosis, as revealed by anti-CD18 and collagen 1 and 3 picrosirius staining, respectively, the hearts of surviving *Stat3<sup>C/C</sup>/C5<sup>-/-</sup>* and *Stat3<sup>C/C</sup>/C3<sup>-/-</sup>/C5<sup>-/-</sup>* mice were indistinguishable from their wild-type CTRLs.

#### Liver-Specific Knockdown of Either C3 or STAT3 Significantly Impairs Myocarditis Development in *Stat3<sup>C/C</sup>* Mice

Since our genetic experiments unequivocally demonstrated the central role of the complement system in the pathogenesis of immune-mediated myocarditis in *Stat3<sup>C/C</sup>* mice, we decided to test the hypothesis that STAT3 activity and complement C3 hyperproduction in the liver are crucial for disease development. To this end, we generated anti-murine C3 or Stat3 siRNAs, appropriately modified to improve their stability, and assembled them with lipidoid particles suitable for *in vivo* delivery. Due to the size and other physicochemical characteristics of the nanoparticles, this formulation is reported to specifically deliver its cargo to tissues characterized by fenestrated capillaries and particularly to the liver upon systemic administration.<sup>21–23</sup> As shown in Figure S2, both C3 and Stat3 siRNAs triggered significant downregulation of the respective mRNA in the liver but not in the spleen, heart, or whole blood. Moreover, the Stat3 siRNA also significantly reduced hepatic C3 mRNA levels, confirming STAT3 dependency of liver C3 expression. Strikingly, when administered to *Stat3<sup>C/C</sup>* newborn mice, both siRNA formulations were able to abolish myocarditis development in more than 50% of the mice compared to a CTRL-unrelated siRNA, as shown by the Kaplan Meyer curve of Figure 3A. Similar to what was already observed with C3 and C5 genetic depletion and previously with IL-6R or complement neutralization,<sup>17</sup> we noticed an “all or nothing” effect. Whereas the mice developing the disease displayed high anti-myosin antibody levels, abundant heart infiltration, and consistent fibrotic damage, similar to those treated with

the CTRL siRNA (Figures 3B and 3C), healthy mice never developed detectable anti-myosin IgGs, inflammatory infiltration, or fibrosis.

#### Liver Knockdown of Either C3 or STAT3 Prevents Myocarditis Development in the EAM Model

We have previously demonstrated that systemic STAT3 inhibition could both prevent and partially cure myocarditis and heart failure in the EAM model.<sup>17</sup> In order to test whether specific inhibition of STAT3 activity in the liver could elicit similar effects and to assess the role of liver-produced C3, we triggered EAM in BALB/c mice and silenced either Stat3 or C3 mRNAs with their specific lipidoid-siRNA nanoparticles, starting from the day of immunization (Figure 4A). As expected, at the end of the experiment, cardiac contractility was severely impaired in mice treated with a CTRL siRNA, as evidenced by a significant reduction of fractional shortening (FS) and ejection fraction (EF), respectively, compared to day 0 (Figures 4B and 4C; empty gray bars). Strikingly, mice treated with either siC3 or siStat3 had instead completely preserved FS and EF at day 28 (Figures 4B and 4C; filled orange or purple bars, respectively), demonstrating that both siRNAs prevent the development of systolic dysfunction. Accordingly, anti-myosin antibodies were much less abundant in mice treated with either siRNA (Figure S3). Circulating C3 was undetectable upon liver C3 silencing until day 21, when the siRNA effects started to decrease, leading to C3 levels comparable to the CTRLs at day 28 (Figure S3).

#### Liver Knockdown of Either C3 or STAT3 Can Therapeutically Alleviate Myocarditis in EAM Mice

In order to assess the therapeutic potential of liver STAT3 or C3 neutralization, the siRNA treatments were started at day 21 (C3) or 28 (Stat3) of the EAM protocol, depending on when systolic dysfunction was first detected (Figure 5A). Strikingly, heart contractility improved much quicker upon treatment with both siRNAs as compared to CTRL-treated mice (Figures 5B and 5C). Whereas in animals treated with siCTRL, systolic dysfunction persisted until the end of the experiment (day 42; Figures 5B and 5C; empty gray bars), and treatment with siC3 completely restored cardiac contractility to the physiological day 0 levels already by day 28, i.e., after 1 week of treatment (Figure 5B; filled orange bars). In Stat3 siRNA-treated mice (Figure 5C; filled purple bars), the recovery of both FS and EF was slower and became evident 2 weeks after the start of the treatment (day 42). Together with the results of the preventive protocol, our experiments clearly show that activity and expression of both Stat3 and C3 in the liver are crucial in the development and progression of EAM, with potentially profound implications also for the human disease.

## DISCUSSION

Myocarditis is a complex disease with different therapeutic options depending on the etiology and on histological, microbiological, and immune features.<sup>4,24</sup> In particular, it can be classified as the following (1) viral, when histological evidence of myocarditis is coupled to viral genome detection, amenable to antiviral drug

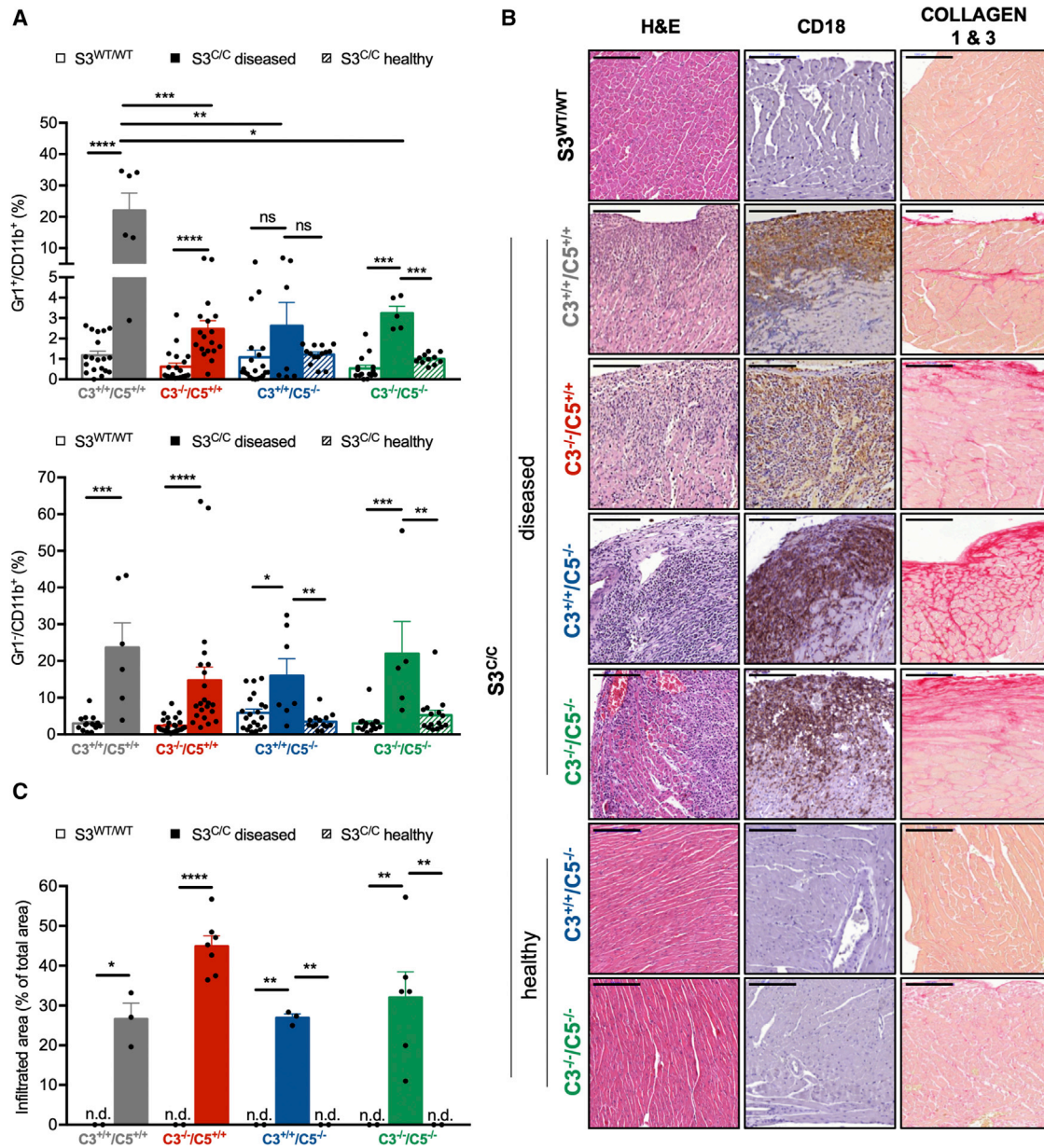


**Figure 2. Reduced Heart Infiltration and Damage in Healthy C5<sup>-/-</sup> and C3<sup>-/-</sup>/C5<sup>-/-</sup> Stat3<sup>C/C</sup> Mice**

Heart infiltration was analyzed by flow cytometry and immunohistochemistry in mice of the different genotypes, described in Figure 1, either healthy (striped bars) or diseased (filled bars). (A) Heart-infiltrating CD11b<sup>+</sup> cells, either positive or negative for Gr1, were analyzed by flow cytometry. Data are mean ± SEM of the indicated values. Mann-Whitney U test, \*p < 0.05; \*\*p < 0.01; \*\*\*p < 0.001; \*\*\*\*p < 0.0001; ns, not significant. (B) Hearts were dissected, formalin fixed, sectioned, and analyzed by hematoxylin and eosin (H&E), CD18 antibody (pan-monocyte marker), or picrosirius red staining (collagen 1 and 3). Scale bars, 100 μm. Representative samples are shown. (C) The infiltrated area was measured on H&E sections in at least 3 mice/group and expressed as percentage of heart area, as described in Materials and Methods. Data are mean ± SEM of the indicated values. n.d., not detected. Unpaired two-tailed Student's t test with Welch's correction, \*p < 0.05; \*\*p < 0.01, \*\*\*\*p < 0.0001.

treatment; (2) autoimmune, i.e., viral negative, with or without circulating cardiac antibodies, where immunosuppressant therapies have shown efficacy;<sup>3,4</sup> or (3) viral and autoimmune, positive both for cardiac antibodies and virus. Among the outstanding questions in myocarditis pathogenesis are the determinants of progression to chronic autoimmune disease, which

occurs in about 30%–40% of patients, and the identification of therapeutic options for viral and autoimmune myocarditis, where immunosuppression is not applicable.<sup>3,4</sup> A better understanding of the pathogenetic mechanisms and of the molecules involved is therefore crucial to help to identify novel personalized, therapeutic approaches.

The group of Rose<sup>12</sup> has demonstrated that complement C3 is required for the inductive phase of EAM. Accordingly, our genetic experiments support a role for complement in the pathogenesis of the immune-mediated myocarditis in *Stat3<sup>C/C</sup>* mice. However, C3 genetic depletion in these mice only delays disease onset without affecting its morbidity. Despite the absence of C3, however, activated C5a can be detected at similar concentrations in both C3-null and C3-sufficient *Stat3<sup>C/C</sup>* mice, suggesting that C5 activation, which has already been proposed to occur in the C3 null mice as a compensatory mechanism,<sup>20</sup> is involved in disease development. In keeping with this observation, C5 gene inactivation leads to a more significant delay in myocarditis onset, completely protecting about 25% of the mice. Disease protection more than doubles in the C3, C5 double-mutant mice, supporting the view that both C3 and C5 activations are involved and suggesting a role for both C3 and C5 anaphylotoxins in addition to the complement cascade.

Our working hypothesis proposed that amplification of IL-6 signaling with constitutive STAT3 activation in the liver plays a major role in myocarditis development of the *Stat3<sup>C/C</sup>* mice.<sup>17</sup> The present study formally proves this view, since abolishing STAT3 liver expression by means of a systemically delivered hepato-specific siRNA was sufficient to significantly protect mice from myocarditis development. Also, liver-specific C3 silencing was effective in blocking disease development, demonstrating that C3 excessive production in the liver, downstream of STAT3 activation, is involved in triggering myocarditis in these mice. Under this regard, C3 silencing was actually strikingly more effective than C3 gene inactivation, probably due to the well-known phenomenon of genetic compensation.<sup>25</sup>

We have previously shown that *in vivo* systemic inhibition of STAT3 was sufficient to both prevent disease development and exert therapeutic effects in the EAM model.<sup>17</sup> Strikingly, our experiments show that the pathogenic role of STAT3 mainly takes place in the liver, not only in the *Stat3<sup>C/C</sup>* mice but also in EAM, since the hepato-specific Stat3 siRNA acted similarly to the systemic inhibitor in impairing myocarditis onset and in ameliorating cardiomyopathy. Remarkably, the targeting of STAT3-activated liver C3 with a similar siRNA formulation also exerted both preventive and therapeutic effects, in partial contrast with previous data suggesting that C3 production is only fundamental in the early phases of EAM onset.<sup>12</sup> This discrepancy might be due to the different strains and treatments used, *CR<sup>-/-</sup>* or *+/+* A/J mice, and cobra venom factor in the cited study versus *C3<sup>-/-</sup>* or *+/+* BALB/c mice and liver-specific siRNAs here.

The link between dysregulation of liver activities and heart inflammation/autoimmunity might well be relevant also in patients, since we have previously shown that IL-6, the main STAT3 activator, as well as C3 and C-reactive protein (CRP), which is universally used in the clinics as an inflammation marker and is capable of activating the complement system, are elevated in the blood of myocarditis patients.<sup>17</sup> Interestingly, IL-6 and STAT3 play a fundamental role in the activation of the liver acute-phase response (APR),<sup>26</sup> which is triggered by both systemic and localized inflammation and consists

of the upregulation of many liver-produced plasma proteins involved in innate immunity, including several complement components and CRP.<sup>27,28</sup> In light of this knowledge, since the liver APR is profoundly implicated in the correct development of acquired immunity, the unexpected link that we observed between liver STAT3 activity and the development of immune-mediated myocarditis is perhaps not too surprising and might be worth exploring in other autoimmune diseases, where both IL-6 and STAT3 have been amply, functionally implicated.<sup>29</sup> Importantly, STAT3 is known to exert a protective role in the heart,<sup>30</sup> suggesting that its systemic inhibition, particularly in heart disease, might compromise cardiomyocyte survival and function and may not be suitable to treat myocarditis. Additionally, although efficient STAT3 inhibitors have been the object of intense research for years, so far, no lead molecule has reached the clinic. In this context, liver-specific siRNA delivery is an attractive approach, since our particle formulation is analogous to that of Onpattro (patisiran), the first-ever siRNA-based drug approved.<sup>31</sup> Indeed, transcription factors are traditionally considered undruggable due to their nuclear localization and the lack of enzymatic activity that could be targeted by small molecules.<sup>32</sup> In contrast an siRNA-mediated approach, targeting not the protein but its mRNA, has the potential to be extremely effective. Another viable option is offered by the effectiveness of the liver C3 siRNA. Indeed, the systemic inhibition of complement functions might be toxic by interfering with native and acquired immunity, whereas the abolishment of C3 production, specifically in the liver, not affecting the other sources of complement proteins, should not exert a generic, immunosuppressive effect and might be a particularly appealing approach for patients with viral and autoimmune myocarditis, where immunosuppression is not supported. One could even envisage combined C3 and Stat3 siRNA-mediated targeting to increase the effectiveness of the treatment. Although the administration of Onpattro in patients is accompanied with a cocktail of anti-inflammatory drugs at the time of treatment, to reduce the risk of infusion-related reactions observed with other liposomal products,<sup>33</sup> it is unlikely that these drugs may alter the overall efficacy of the Stat3 and C3 siRNAs, which are expected to be long lasting. Indeed, we did not detect any sign of toxicity, including body weight loss, in any of the EAM groups.

The nonredundant pathogenic role that we have uncovered for liver-produced complement factors in myocarditis pathogenesis is in line with the well-known complement vital functions in both coronary disease and heart failure. Our data suggest that high levels of complement proteins, in particular, C3, and of complement activation, either of reactive origin or genetically determined, may serve as biomarkers to predict the progression from acute to chronic myocarditis.<sup>4</sup> In keeping with this idea, C3, C3a, C5, and Membrane Attack Complex (MAC) complex levels are known to correlate with systemic, low-grade inflammation.<sup>34</sup> Our findings are therefore compatible with the hypothesis that a pre-existing, even undetected inflammatory condition, raising IL-6 activity, may trigger constitutive liver STAT3 activation and consequent initiation of the APR. This would result in increased circulating levels of complement factors and other APR proteins, such as CRP, which may facilitate complement activation

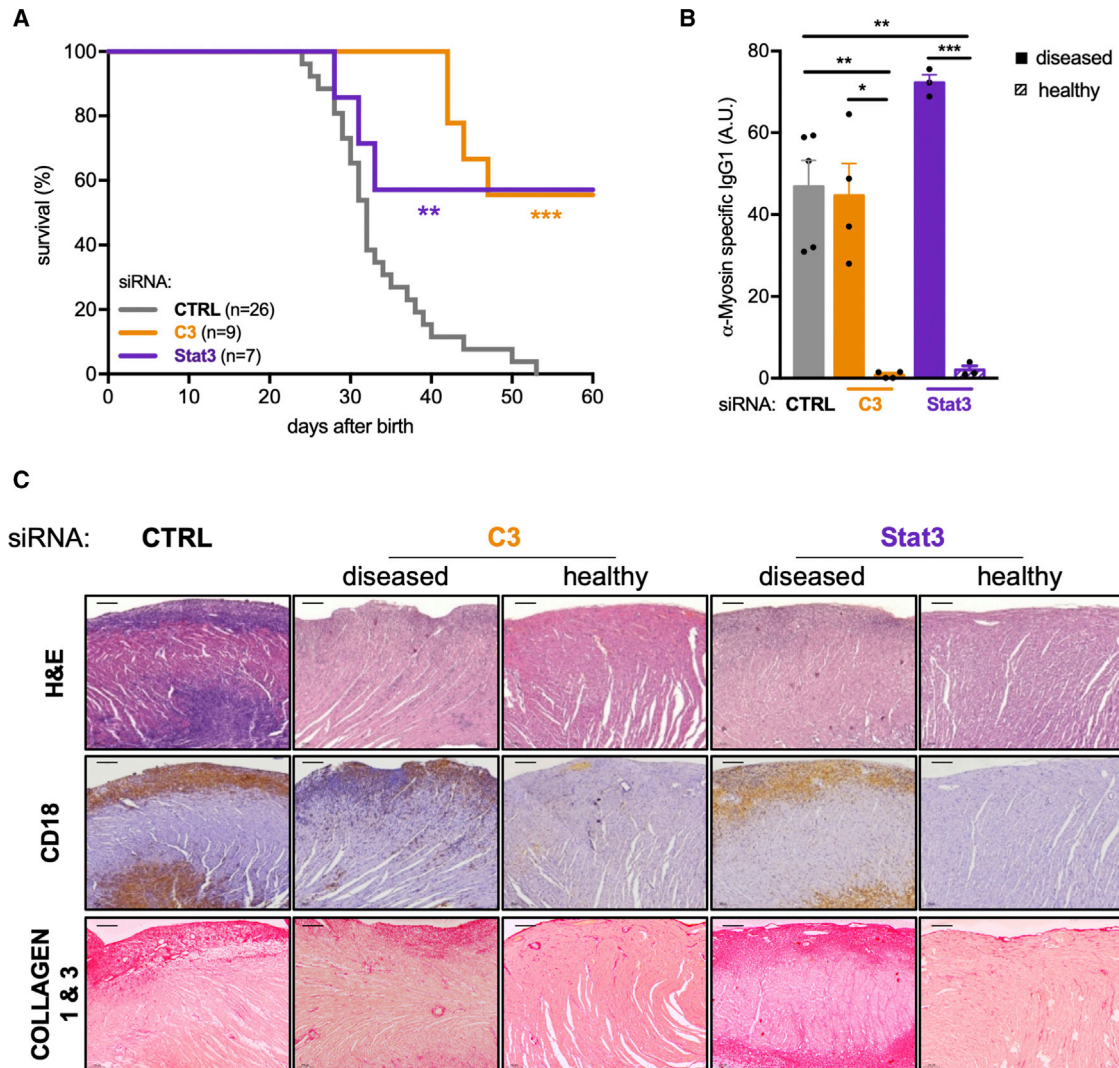


**Figure 3. siRNA-Mediated Liver-Specific Downregulation of C3 or Stat3 Can Prevent Myocarditis in Stat3<sup>C/C</sup> Mice**

Newborn Stat3<sup>C/C</sup> mice were injected i.p. (from postnatal day 0 to 21) and then i.v. every 3 days with siRNA control (CTRL), against C3 or against Stat3, followed by serum withdrawal and heart analysis, as described below. (A) The Kaplan Meyer curve shows survival of Stat3<sup>C/C</sup> mice injected with siRNA CTRL (gray line, n = 26), against C3 (orange line, n = 9) or against Stat3 (purple line, n = 7). Log rank Mantel-Cox test, p values: CTRL siRNA versus C3 siRNA, \*\*\*p < 0.001; CTRL siRNA versus Stat3 siRNA, \*\*p < 0.01. (B) Serum anti-myosin IgG1 autoantibodies were measured by ELISA in mice treated with CTRL siRNA (gray bar); C3 siRNA, either diseased (filled orange bar) or healthy (striped orange bar); and Stat3 siRNA, either diseased (filled purple bar) or healthy (striped purple bar). Data are mean ± SEM. Unpaired two-tailed Student's t test with Welch's correction, \*\*p < 0.01; \*\*\*p < 0.001. (C) The hearts of mice belonging to the above groups were sectioned and analyzed by H&E, CD18 antibody (pan-monocyte marker), or picrosirius red staining (collagen 1 and 3). Scale bars, 100 μm.

and deposition in a heart, potentially already damaged by viral infection, and help start autoimmunity and chronic heart inflammation.

Further work analyzing patients at the time of symptoms onset, during therapy and after recovery, is required to support the feasibility of translating our therapeutic protocols to the clinic. In particular, the systemic and local levels of complement proteins, such as C3, C5, C3a, and C5a; their deposition on heart tissue; and the concentrations of IL-6 and CRP, will have to be assessed and analyzed with reference with the clinical history of the patient, keeping also into

account the differences between the murine and human complement systems.<sup>35</sup> We predict that our protocol may represent a much-needed therapeutic option for those patients with viral and autoimmune myocarditis who cannot benefit from standard immunosuppressive treatment.

## MATERIALS AND METHODS

### Animals and Analysis

Generation of the Stat3<sup>C/C</sup> mice was previously described.<sup>36</sup> Mice were crossed for 8 generations in the BALB/c background. C3<sup>-/-</sup>

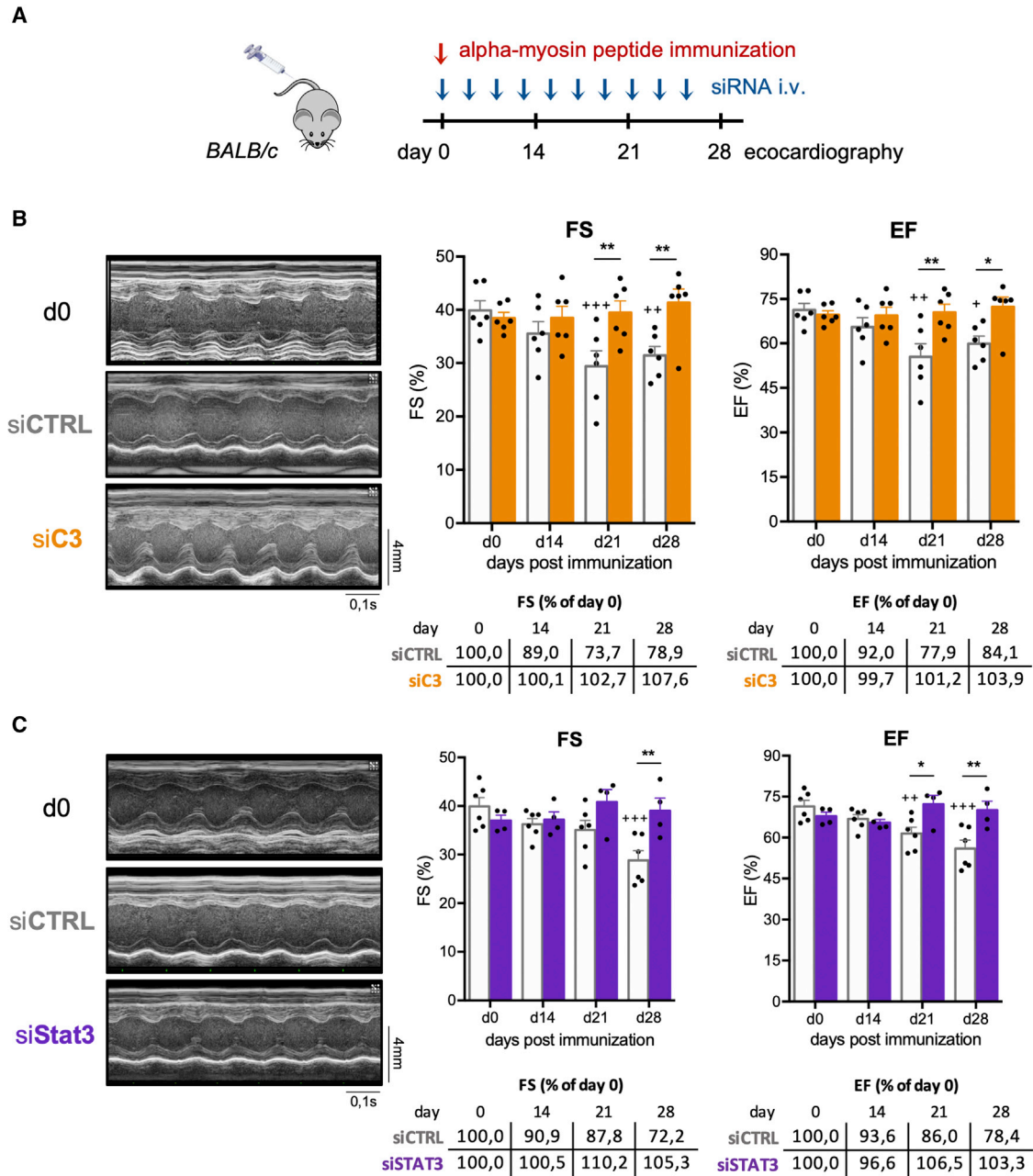


**Figure 4. C3 or Stat3 siRNA Treatment Prevents EAM Development in BALB/c Mice**

(A) Schematic representation of the experiment. BALB/c mice were immunized with an alpha-myosin peptide; treated i.v. every 3 days with CTRL or specific siRNAs, starting from day 0; and sacrificed at day 28. (B and C) Echocardiographic analyses were performed at the indicated days postimmunization, followed by calculation of the fractional shortening (FS) and ejection fraction (EF). Selected Doppler images are shown at day 0 (untreated CTRLs) and day 28 after immunization. The histograms show mean  $\pm$  SEM values of 6 mice/group. Statistical differences were calculated by two-way ANOVA on repeated measures with Bonferroni post-test. + indicates differences between day 0 and the indicated time points of the same siRNA treatment; \* indicates differences between CTRL and specific siRNA groups at the indicated time point. +, \*p < 0.05; ++, \*\*p < 0.01; +++p < 0.001. Tables below the histograms report the percentages of FS and EF, calculated at each time point, with respect to the values at day 0. (B) Mice were injected with either CTRL (siCTRL, empty gray bars) or C3 siRNA (siC3, filled orange bars). (C) Mice were injected with either CTRL (siCTRL, empty gray bars) or Stat3 siRNA (siStat3, filled purple bars).

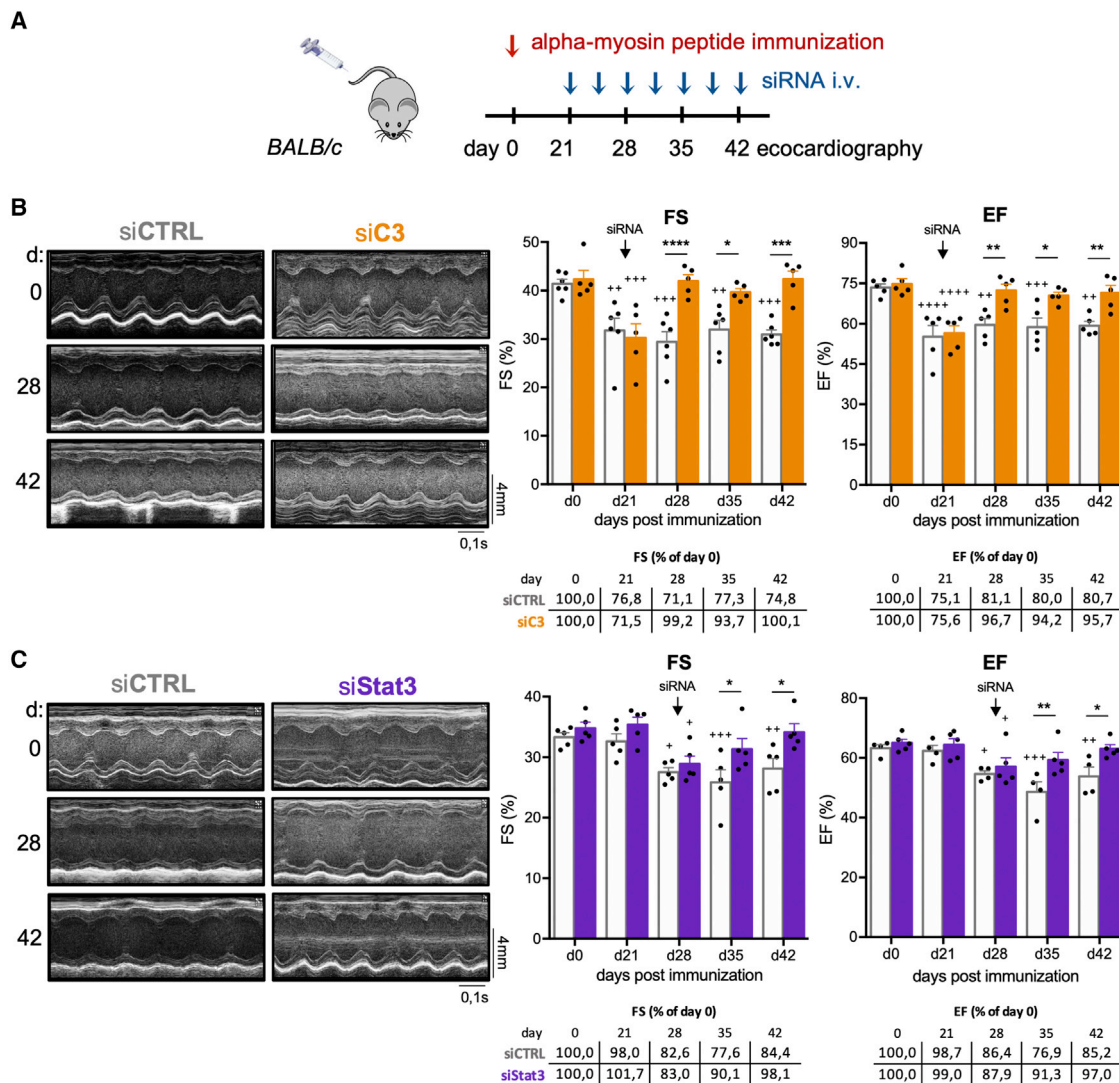


**Figure 5. C3 or Stat3 siRNA Treatment Rescues Systolic Dysfunction in EAM.**

(A) Schematic representation of the experiment. BALB/c mice were immunized with an alpha-myosin peptide as in Figure 4; injected i.v. with CTRLs or specific siRNAs every 3 days starting from day 21 (C3, B) or 28 (Stat3, C), when echocardiographic analyses showed systolic dysfunction; and sacrificed at day 42. (B and C) Echocardiographic analyses were performed at the indicated times (days postimmunization), followed by calculation of the FS and EF. Selected Doppler images are shown at day 0 (untreated CTRLs) and day 28 and day 42 after immunization. The histograms show mean  $\pm$  SEM of the values. Statistical differences were calculated by two-way ANOVA on repeated measures with Bonferroni post-test. + indicates differences between day 0 and the indicated time points of the same siRNA treatment; \* indicates differences between CTRL and specific siRNA groups at the indicated time point. +, \* $p$  < 0.05; ++, \*\* $p$  < 0.01; +++, \*\*\* $p$  < 0.001; +++++, \*\*\*\* $p$  < 0.0001. Tables below the histograms report the percentages of FS and EF calculated at each time point with respect to the values at day 0. (B) Mice were injected with either CTRL (siCTRL, empty gray bars) or C3 siRNA (siC3, filled orange bars). (C) Mice were injected with either CTRL (siCTRL, empty gray bars) or Stat3 siRNA (siStat3, filled purple bars).

and  $C5^{-/-}$  mice were kindly supplied by Prof. Federica Cavallo (University of Turin) and Marina Botto (Imperial College of London). Mice were maintained in the transgenic unit of the Molecular Biotechnology Center (University of Turin) under a 12-h light-dark cycle and provided food and water *ad libitum*, inspected and weighed every 3 days. Procedures were in conformity with national and international laws and policies, as approved by the Faculty Ethical Committee.

### Flow Cytometry

To isolate infiltrating cells, hearts were disaggregated with collagenase type 2 (cat. C6885; Sigma-Aldrich, St. Louis, MO, USA) and protease type XIV (cat. P5147; Sigma-Aldrich, St. Louis, MO, USA), as described.<sup>17</sup> Cells were stained with fluorescein isothiocyanate (FITC) anti-Gr1 (cat. 108405; BioLegend, San Diego, CA, USA) and phycoerythrin (PE) anti-CD11b antibodies (cat. 101208; BioLegend, San Diego, CA, USA), diluted 1:100 (30  $\mu$ L per staining)



for 20 min at 4°C, and analyzed with a FACSCalibur flow cytometer (BD Biosciences, Franklin Lakes, NJ, USA) and CellQuest software.

### Experimental Autoimmune Myocarditis

8-week-old female BALB/c mice were immunized as described<sup>37</sup> with the alpha-myosin heavy-chain peptide (Myhc-alpha)<sub>614-634</sub> (cat. 62554; AnaSpec, Fremont, CA, USA), emulsified 1:1 in Freund's complete adjuvant (CFA; cat. BD 263810; Difco Laboratories, Detroit, MI, USA). In the preventive setting (Figure 4), siRNA lipidoid nanoparticles were administered starting from the first day of immunization, and disease progression was monitored by echocardiography. For the therapeutic setting (Figure 5), all EAM mice were subjected to echocardiography at days 21–28 to assess disease development. Mice showing a reduction of at least 10% in EF and FS were recruited for siRNA injection and randomized into the CTRL and treated groups in order to obtain homogeneous cohorts. No animals were excluded after starting the siRNA treatments in either protocol. Throughout the entire experiments, mice weight was monitored, without the observation of any weight loss or other visible signs of distress.

### In Vivo siRNA-Containing Lipidoid Nanoparticle Treatment

Lipidoid siRNA formulations were developed by Alnylam Pharmaceuticals (Cambridge, MA) as described,<sup>22</sup> using a three-component systemic siRNA delivery system, based on the lipid-like material C12-200,<sup>38</sup> cholesterol, and the poly(ethylene glycol) (PEG) lipid mPEG2000-C14 glyceride. Mouse reference sequences for Stat3 mRNA (GenBank: NM\_213659) and C3 mRNA (GenBank: NM\_009778) were used for siRNA selection. Candidate siRNA sequences were subjected to a homology search against the RefSeq mRNA database and ranked the most specific siRNAs against each target for synthesis. Single-stranded RNAs were synthesized at Alnylam Pharmaceuticals on controlled pore glass using standard phosphoramidite chemistry as described elsewhere.<sup>39</sup> The following strands were used: C3 sense strand: cGAucAGuucAGucGAuuudTdT; C3 antisense strand: AAAUCGACUGAACUGAUCGdTsdT; Stat3 sense strand: GccuAAGAuGAccuAGAdTsdT; Stat3 antisense strand: UCuAGGUCAAUCUUGAGGCdTsdT; CTRL sense strand: cuuAcGcuGAGuAcuucGAdTsdT; CTRL antisense strand: UCGAA GuACUcAGCGuAAGdTsdT; 2'-OMe-modified nucleotides are in lowercase; s is phosphorothioate linkage. The formulation developed is hepato-specific (>90% injected dose distributes to liver) and can induce fully reversible gene silencing. Newborn *Stat3<sup>C/C</sup>* mice were injected intraperitoneally (i.p.) with 1 mg/kg of C3, Stat3, or CTRL siRNA-containing nanoparticles,<sup>22</sup> every 3 days, starting from post-natal days 1 to 21, and subsequently, intravenously (i.v.) with 0.1 mg/kg (C3) or 0.5 mg/kg (Stat3, CTRL). Diseased and healthy animals were defined based on observational data (body weight loss, body stance, activity, sudden death), followed by retrospective serological and immunohistochemistry (IHC) analysis.

### ELISA Assays

Anti-cardiac alpha-myosin IgG1 levels were measured upon coating with 3 µg/mL of cardiac myosin, prepared as described,<sup>40</sup> followed by incubation with mouse sera and horseradish peroxidase (HRP)-

labeled rat anti-mouse IgG1 (cat. 559626; BD Biosciences). Murine C3 was captured with a polyclonal goat IgG to mouse C3 and revealed with the same antibody peroxidase conjugated (cat. 55557; Cappel, ICN Pharmaceuticals, Costa Mesa, CA, USA). SAP (serum amyloid P) component, normal mouse standard (cat. 565193; Calbiochem, San Diego, CA, USA), was used as a standard, according to the manufacturer's instructions. Circulating C3a and C5a levels were measured using BD Biosciences assays (Franklin Lakes, NJ, USA), according to the manufacturer's instructions. Briefly, coating was performed with 1.5 µg/mL (C3a, cat. 558250) and 2 µg/mL (C5a, cat. 558027) antibodies overnight at 4°C; then, diluted sera (1:2,000 for C3a; 1:50 for C5a) were incubated for 2.5 h at room temperature, and biotinylated antibodies (C3a, cat. 558251; C5a, cat. 558028) were used for detection of the assays, developed with a biotin-streptavidin system (cat. 554066). Reference curves for C3a and C5a were made by serial dilution of purified mouse recombinant proteins (cat. C3: 558618; C5a: 622597; Pharmingen, Franklin Lakes, NJ, USA).

### Histological and Immunohistochemical Analysis

Hearts were fixed in 4% paraformaldehyde for 24 h and paraffin embedded. Independent sections were produced as follows: 5 adjacent 6 µm sections were generated, followed by removal of a 50-µm-thick portion of the paraffin sample block, generation of further 5 adjacent 6 µm sections, removal, and so on for at least 5 rounds. One random section from each layer was then stained with hematoxylin and eosin. For immunohistochemistry, antigen retrieval on formalin-fixed paraffin-embedded (FFPE) sections was performed with citrate buffer (Sigma-Aldrich), and sections were then saturated (3% BSA + 5% goat serum in Tris-buffered saline [TBS]); incubated overnight with rat anti-mouse CD18 (cat. T-2122; BMA Biomedicals, Augst, Switzerland), followed by biotinylated anti-rat IgG (cat. BA-2000; Vector Laboratories) and avidin-biotin (ABC)-HRP complex (cat. PK-4000; Vector Laboratories); and developed with 3,3'-diaminobenzidine tetrahydrochloride (DAB) substrate (sub: cat. 11718096001; Roche Diagnostics, Mannheim, Germany). Collagen fibers were evidenced by picrosirius red staining (cat. 365548; Sigma-Aldrich, St. Louis, MO, USA). Images were acquired with the Panoramic Desk (3D Histech, Budapest, Hungary). The infiltrated area was measured with Fiji software on hematoxylin-and-eosin-stained sections. Five independent, 10× images per heart were randomly acquired and quantified; the infiltrated area is expressed as percentage of total area.

### Real-Time PCR

Total RNA was prepared with the Trizol protocol (cat. 15596026; Invitrogen, Carlsbad, CA, USA), RNA was treated with DNase, and reverse transcription was performed with the High-Capacity cDNA Reverse Transcription Kit, according to the manufacturer's instruction (cat. 4368814; Applied Biosystems, Carlsbad, CA, USA). qRT-PCR reactions were performed, as previously described, using the Universal Probe Library system (Roche Diagnostics, Mannheim, Germany) and Platinum Quantitative PCR SuperMix-UDG w/ROX (cat. 11743500; Invitrogen, Carlsbad, CA, USA). Probes and oligonucleotide sequences used are reported in the Table S1. The 18S rRNA predeveloped TaqMan assay (cat. 4319413; Applied Biosystems,

Carlsbad, CA, USA) was used as an internal control. PCR protocol is 50°C for a 2-min hold, 95°C for a 2-min hold, and 40 cycles of 95°C, 15 s; 60°C, 30 s.

### Echocardiography

Echocardiography was performed in mice anesthetized with 1% isoflurane with a Vevo2100 High-Resolution Imaging System (Visual Sonics, Toronto, ON, Canada) with the transducer MS550D when heart rate was  $\approx$  450 beats per minute (bpm). Left-ventricle end-systolic and left-ventricle end-diastolic (LVES and LVED, respectively) diameters were measured with the 2D long-axis left-ventricle M-mode. FS was calculated as  $(LVED - LVES)/LVED\%$ . EF was calculated using Doppler images as stroke volume/end-diastolic volume (SV/EDV), expressed as a percentage at the indicated days after the first immunization. Results are shown as mean  $\pm$  SEM.

### Statistics

Shapiro-Wilk normality test has been performed on all data and nonparametric analysis (Mann-Whitney U test) used when needed (Figures 1A and 2A). For normally distributed data, the unpaired two-tailed Student's t test with Welch's correction was used for comparisons between two groups of samples. Two-way ANOVA on repeated measures with Bonferroni post-test was used for comparison of group/time in all echocardiographic analyses. The log rank Mantel-Cox test was used for significance of survival curves. For all of the experiments, mean values per group and corresponding intervals of confidence were calculated and reported in Table S2 (experiments in Figures 1, 2, and 3) and in Table S3 (experiments in Figures 4 and 5). All statistical analyses were performed with GraphPad Prism 7.0a (GraphPad Software). p values lower or equal to 0.05 were considered significant.

### SUPPLEMENTAL INFORMATION

Supplemental Information can be found online at <https://doi.org/10.1016/j.omtm.2020.05.023>.

### AUTHOR CONTRIBUTIONS

Conception and design, V.P.; Development of Methodology, L.A., F.M., A.C., D.V., C.G., and R.L.B.; Acquisition of Data and Reagents Provision (provided animals, acquired fluorescence-activated cell sorting (FACS) data, performed echocardiography analysis, provided facilities, developed essential reagents, etc.), S.B., L.C., J.C., C.Z., R.L.B., F.C., and V.K.; Analysis and Interpretation of Data (e.g., statistical analysis, biostatistics, computational analysis, histology), L.A., F.M., M.F., A.G., and P.P.; Writing of the Manuscript, V.P., L.A., and F.M.; Study Supervision, V.P.

### CONFLICTS OF INTEREST

The authors declare no competing interests.

### ACKNOWLEDGMENTS

The authors thank Prof. Marina Botto for kindly providing complement C5 knockout mice, Dr. Marta Gai for help with image analysis,

and Profs. Emilio Hirsch and Mara Brancaccio for critically reading the manuscript. siRNA duplexes and their lipid nanoformulations were provided by Alnylam Pharmaceuticals Inc., Cambridge, MA. This work was supported by the Fondazione CRT, Italian Cancer Research Association (AIRC; IG16930 to V.P.), Italian Ministry of University and Research (MIUR PRIN 2015 YYLBTR to P.P.), and a Truus and Gerrit van Riemsdijk Foundation, Liechtenstein, donation to V.P.

### REFERENCES

- Schultheiss, H.P., Kühl, U., and Cooper, L.T. (2011). The management of myocarditis. *Eur. Heart J.* 32, 2616–2625.
- Caforio, A.L., Mahon, N.J., Tona, F., and McKenna, W.J. (2002). Circulating cardiac autoantibodies in dilated cardiomyopathy and myocarditis: pathogenetic and clinical significance. *Eur. J. Heart Fail.* 4, 411–417.
- Frustaci, A., Russo, M.A., and Chimenti, C. (2009). Randomized study on the efficacy of immunosuppressive therapy in patients with virus-negative inflammatory cardiomyopathy: the TIMIC study. *Eur. Heart J.* 30, 1995–2002.
- Caforio, A.L., Pankuweit, S., Arbustini, E., Basso, C., Gimeno-Blanes, J., Felix, S.B., Fu, M., Heliö, T., Heymans, S., Jahns, R., et al. (2013). Current state of knowledge on aetiology, diagnosis, management, and therapy of myocarditis: a position statement of the European Society of Cardiology Working Group on Myocardial and Pericardial Diseases. *Eur. Heart J.* 34, 2636–2648d.
- Neumann, D.A., Lane, J.R., Wulff, S.M., Allen, G.S., LaFond-Walker, A., Herskowitz, A., and Rose, N.R. (1992). In vivo deposition of myosin-specific autoantibodies in the hearts of mice with experimental autoimmune myocarditis. *J. Immunol.* 148, 3806–3813.
- Ciháková, D., Sharma, R.B., Fairweather, D., Afanasyeva, M., and Rose, N.R. (2004). Animal models for autoimmune myocarditis and autoimmune thyroiditis. *Methods Mol. Med.* 102, 175–193.
- Poli, V., Bruno, K.A., and Fairweather, D. (2020). Autoimmune myocarditis: animal models. In *Myocarditis*, A.L. Caforio, ed. (Springer Nature), pp. 111–127.
- Barin, J.G., and Čiháková, D. (2013). Control of inflammatory heart disease by CD4+ T cells. *Ann. N Y Acad. Sci.* 1285, 80–96.
- Gao, S., Ho, D., Vatner, D.E., and Vatner, S.F. (2011). Echocardiography in Mice. *Curr. Protoc. Mouse Biol.* 1, 71–83.
- Eriksson, U., Kurrer, M.O., Schmitz, N., Marsch, S.C., Fontana, A., Eugster, H.P., and Kopf, M. (2003). Interleukin-6-deficient mice resist development of autoimmune myocarditis associated with impaired upregulation of complement C3. *Circulation* 107, 320–325.
- Fairweather, D., and Cihakova, D. (2009). Alternatively activated macrophages in infection and autoimmunity. *J. Autoimmun.* 33, 222–230.
- Kaya, Z., Afanasyeva, M., Wang, Y., Dohmen, K.M., Schlichting, J., Tretter, T., Fairweather, D., Holers, V.M., and Rose, N.R. (2001). Contribution of the innate immune system to autoimmune myocarditis: a role for complement. *Nat. Immunol.* 2, 739–745.
- Veldhoen, M., Hocking, R.J., Atkins, C.J., Locksley, R.M., and Stockinger, B. (2006). TGFbeta in the context of an inflammatory cytokine milieu supports de novo differentiation of IL-17-producing T cells. *Immunity* 24, 179–189.
- Harris, T.J., Grosso, J.F., Yen, H.R., Xin, H., Kortylewski, M., Albesiano, E., Hipkiss, E.L., Getnet, D., Goldberg, M.V., Maris, C.H., et al. (2007). Cutting edge: An in vivo requirement for STAT3 signaling in TH17 development and TH17-dependent autoimmunity. *J. Immunol.* 179, 4313–4317.
- Baldeviano, G.C., Barin, J.G., Talor, M.V., Srinivasan, S., Bedja, D., Zheng, D., Gabrielson, K., Iwakura, Y., Rose, N.R., and Cihakova, D. (2010). Interleukin-17A is dispensable for myocarditis but essential for the progression to dilated cardiomyopathy. *Circ. Res.* 106, 1646–1655.
- Nindl, V., Maier, R., Ratering, D., De Giuli, R., Züst, R., Thiel, V., Scandella, E., Di Padova, F., Kopf, M., Rudin, M., et al. (2012). Cooperation of Th1 and Th17 cells determines transition from autoimmune myocarditis to dilated cardiomyopathy. *Eur. J. Immunol.* 42, 2311–2321.

17. Camporeale, A., Marino, F., Papageorgiou, A., Carai, P., Fornero, S., Fletcher, S., Page, B.D., Gunning, P., Forni, M., Chiarle, R., et al. (2013). STAT3 activity is necessary and sufficient for the development of immune-mediated myocarditis in mice and promotes progression to dilated cardiomyopathy. *EMBO Mol. Med.* *5*, 572–590.
18. Trendelenburg, M., Fossati-Jimack, L., Cortes-Hernandez, J., Turnberg, D., Lewis, M., Izui, S., Cook, H.T., and Botto, M. (2005). The role of complement in cryoglobulin-induced immune complex glomerulonephritis. *J. Immunol.* *175*, 6909–6914.
19. Wetsel, R.A., Fleischer, D.T., and Haviland, D.L. (1990). Deficiency of the murine fifth complement component (C5). A 2-base pair gene deletion in a 5'-exon. *J. Biol. Chem.* *265*, 2435–2440.
20. Huber-Lang, M., Sarma, J.V., Zetoune, F.S., Rittirsch, D., Neff, T.A., McGuire, S.R., Lambris, J.D., Warner, R.L., Flierl, M.A., Hoesel, L.M., et al. (2006). Generation of C5a in the absence of C3: a new complement activation pathway. *Nat. Med.* *12*, 682–687.
21. John, M., Constien, R., Akinc, A., Goldberg, M., Moon, Y.A., Spranger, M., Hadwiger, P., Soutschek, J., Vormlocher, H.P., Manoharan, M., et al. (2007). Effective RNAi-mediated gene silencing without interruption of the endogenous microRNA pathway. *Nature* *449*, 745–747.
22. Akinc, A., Goldberg, M., Qin, J., Dorkin, J.R., Gamba-Vitalo, C., Maier, M., Jayaprakash, K.N., Jayaraman, M., Rajeev, K.G., Manoharan, M., et al. (2009). Development of lipidoid-siRNA formulations for systemic delivery to the liver. *Mol. Ther.* *17*, 872–879.
23. Zeigerer, A., Gilleron, J., Bogorad, R.L., Marsico, G., Nonaka, H., Seifert, S., Epstein-Barash, H., Kuchimanchi, S., Peng, C.G., Ruda, V.M., et al. (2012). Rab5 is necessary for the biogenesis of the endolysosomal system in vivo. *Nature* *485*, 465–470.
24. Maisch, B. (2019). Cardio-Immunology of Myocarditis: Focus on Immune Mechanisms and Treatment Options. *Front. Cardiovasc. Med.* *6*, 48.
25. El-Brolosy, M.A., and Stainier, D.Y.R. (2017). Genetic compensation: A phenomenon in search of mechanisms. *PLoS Genet.* *13*, e1006780.
26. Cray, C., Zaias, J., and Altman, N.H. (2009). Acute phase response in animals: a review. *Comp. Med.* *59*, 517–526.
27. Fattori, E., Cappelletti, M., Costa, P., Sellitto, C., Cantoni, L., Carelli, M., Faggioni, R., Fantuzzi, G., Ghezzi, P., and Poli, V. (1994). Defective inflammatory response in interleukin 6-deficient mice. *J. Exp. Med.* *180*, 1243–1250.
28. Alonzi, T., Maritano, D., Gorgoni, B., Rizzuto, G., Libert, C., and Poli, V. (2001). Essential role of STAT3 in the control of the acute-phase response as revealed by inducible gene inactivation [correction of activation] in the liver. *Mol. Cell. Biol.* *21*, 1621–1632.
29. Camporeale, A., and Poli, V. (2012). IL-6, IL-17 and STAT3: a holy trinity in autoimmunity? *Front. Biosci.* *17*, 2306–2326.
30. Fischer, P., and Hilfiker-Kleiner, D. (2007). Survival pathways in hypertrophy and heart failure: the gp130-STAT axis. *Basic Res. Cardiol.* *102*, 393–411.
31. Mullard, A. (2018). FDA approves landmark RNAi drug. *Nat. Rev. Drug Discov.* *17*, 613.
32. Hagenbuchner, J., and Ausserlechner, M.J. (2016). Targeting transcription factors by small compounds—Current strategies and future implications. *Biochem. Pharmacol.* *107*, 1–13.
33. Tabernero, J., Shapiro, G.L., LoRusso, P.M., Cervantes, A., Schwartz, G.K., Weiss, G.J., Paz-Ares, L., Cho, D.C., Infante, J.R., Alsina, M., et al. (2013). First-in-humans trial of an RNA interference therapeutic targeting VEGF and KSP in cancer patients with liver involvement. *Cancer Discov.* *3*, 406–417.
34. Hertle, E., Stehouwer, C.D., and van Greevenbroek, M.M. (2014). The complement system in human cardiometabolic disease. *Mol. Immunol.* *61*, 135–148.
35. Merle, N.S., Church, S.E., Fremeaux-Bacchi, V., and Roumenina, L.T. (2015). Complement System Part I - Molecular Mechanisms of Activation and Regulation. *Front. Immunol.* *6*, 262.
36. Barbieri, I., Pensa, S., Pannellini, T., Quaglino, E., Maritano, D., Demaria, M., Voster, A., Turkson, J., Cavallo, F., Watson, C.J., et al. (2010). Constitutively active Stat3 enhances neu-mediated migration and metastasis in mammary tumors via upregulation of Cten. *Cancer Res.* *70*, 2558–2567.
37. Sonderegger, I., Röhn, T.A., Kurrer, M.O., Iezzi, G., Zou, Y., Kastelein, R.A., Bachmann, M.F., and Kopf, M. (2006). Neutralization of IL-17 by active vaccination inhibits IL-23-dependent autoimmune myocarditis. *Eur. J. Immunol.* *36*, 2849–2856.
38. Love, K.T., Mahon, K.P., Levins, C.G., Whitehead, K.A., Querbes, W., Dorkin, J.R., Qin, J., Cantley, W., Qin, L.L., Racie, T., et al. (2010). Lipid-like materials for low-dose, in vivo gene silencing. *Proc. Natl. Acad. Sci. USA* *107*, 1864–1869.
39. Frank-Kamenetsky, M., Grefhorst, A., Anderson, N.N., Racie, T.S., Bramlage, B., Akinc, A., Butler, D., Charisse, K., Dorkin, R., Fan, Y., et al. (2008). Therapeutic RNAi targeting PCSK9 acutely lowers plasma cholesterol in rodents and LDL cholesterol in nonhuman primates. *Proc. Natl. Acad. Sci. USA* *105*, 11915–11920.
40. Shiverick, K.T., Thomas, L.L., and Alpert, N.R. (1975). Purification of cardiac myosin. Application to hypertrophied myocardium. *Biochim. Biophys. Acta* *393*, 124–133.